EFFECT OF LiOH, NaOH, AND KOH ON CORROSION AND OXIDE MICROSTRUCTURE OF Zr-BASED ALLOYS

Y.H. JEONG, H.G. KIM, Y.H. JUNG
Korea Atomic Energy Research Institute,
Taejon, Republic of Korea

H. RUHMANN
Siemens AG, Power Generation Group (KWU),
Erlangen, Germany

Abstract

Long-term corrosion test, SIMS analysis, and TEM microstructural study were carried out to investigate the corrosion characteristics and mechanism of Zr alloys in alakli hydroxides. The corrosion tests were performed in solutions of LiOH, NaOH, KOH, RbOH, and CsOH at 350°C for 500 days. SIMS analysis was performed for the specimens prepared to have an equal oxide thickness. TEM studies on the specimens with an equal oxide thickness in various solutions in both pre- and post-transition regimes were also conducted.

The corrosion rate in alkali hydroxide solutions was observed to decrease as the ionic radius of alkali cation was increased. The penetration depth of cation into the oxide decreases with increasing the ionic radius of cation. Even though the oxide thickness was equal, the different oxide morphologies were observed in specimens. Namely, in LiOH solution the oxide morphology was transformed early from columnar to equiaxed structure. However, in KOH solution the columnar structure was maintained up to post-transition regime. Based on the corrosion test, SIMS analysis, and microstructural study, the cation is considered to control the corrosion in a alkali hydroxide solution and its effect is dependent on the concentration of alkali and the oxide thickness. The slight acceleration of the corrosion rate at a low concentration is thought to be caused by cation incorporation into oxide while the significant acceleration at a high concentration is due to the transformation of oxide microstructure that would be induced by cation incorporation. KOH was shown not to affect significantly the corrosion and the hydrogen pickup of Zircaloy. Therefore, it has a potential for PWR application only from the point of view of Zircaloy corrosion.

1. Introduction

LiOH, which is added to control the pH of primary coolant in LWR, has been known to accelerate the corrosion of nuclear fuel cladding. The effect of LiOH on the Zircaloy corrosion has been previously studied by many researchers [1-10]. The Li incorporation into oxide [3,11], the modification of oxide nucleation or growth [12], and the dissolution and reprecipitation of oxide [10] were suggested to be the reasons for the accelerated corrosion in LiOH solution. The content of penetrated Li^+ into oxide was recently measured by SIMS [13-16], and LiOH was suggested to affect the barrier layer of oxide. TEM studies on the oxide were also conducted to investigate the effect of LiOH on the oxide microstructure [13].

Meanwhile, KOH is currently used as a pH controller with other alkali hydroxides in WWER reactors. It was reported that KOH showed high compatibility with Zr-1Nb alloy in in-reactor[17] and the less corrosive characteristic to Zircaloy than LiOH based on the out-of-pile loop test[14]. However, there have been no reports concerning the effect of KOH on Zircaloy corrosion in Western PWR reactors.

In the previous research [11], the corrosion of Zr alloys was investigated in various alkali hydroxide solutions, and the cation incorporation into oxide was suggested to play an important role on the corrosion acceleration. But, only pre-transition corrosion characteristics could be studied for corrosion resistant Zr alloys like Zircaloy due to relatively short exposure time. As a result, the effect of alkali hydroxide on Zircaloy corrosion was not clearly evaluated in the previous study. Therefore, in this study, the corrosion characteristics in equimolar LiOH, NaOH, KOH, RbOH, and CsOH solutions in post-transition as well as pre-transition regime were investigated from long-term corrosion tests (500 days). For the better understanding of cation incorporation, SIMS analysis was performed to observe how Li^+, Na^+, K^+ cation penetrate into the oxide. TEM studies on the oxide were also conducted to investigate the oxide microstructure change induced by the cation incorporation and its effect on corrosion.

2. Experimental Procedure

In this study, two kinds of Zr alloys, that is, Zircaloy-4 and Zr-Sn-Nb alloy, were used for corrosion tests. The chemical compositions of Zircaloy-4 and Zr-Sn-Nb alloys were 1.51wt%Sn, 0.22wt%Fe, and 0.11wt%Cr and 0.8wt%Sn, 0.8wt%Nb, and transition metal (TRM:0.3wt%), respectively. The material condition of both alloys was fully recrystallized. The specimens were chemically polished using a pickling solution before the corrosion test. The corrosion tests were conducted in aqueous alkali solutions in the static autoclave at 350°C under the pressure of 17 MPa. Corrosion resistance was evaluated by measuring the weight gain during the test. According to the literature survey, it is still controversial which one, anion or cation, plays an important role on the corrosion of Zircaloy in alkali solutions. Therefore, the corrosion tests were performed in LiOH, NaOH, KOH, RbOH, and CsOH solutions of 4.3mmol and 32.5mmol with equimolar M^+ and OH^-, where 4.3 mmol corresponds to 30 ppm Li, 99 ppm Na, 169 ppm K, 360 ppm Rb, and 574 ppm Cs and 32.5 mmol corresponds to 220 ppm Li, 724 ppm Na, 1231 ppm K, 2692 ppm Rb, and 4186 ppm Cs.

The penetrations of Li^+, Na^+, and K^+ into the oxides formed in LiOH, NaOH, and KOH solutions were investigated by SIMS analysis to clarify the relationship between cation radius and cation incorporation. Cameca-ims 4f SIMS was used for the analysis of the cation in the oxide. Primary ion beam of O^{2+} was used because the sensitivity is improved for the secondary ion detection of Li^+, Na^+, and K^+. The acceleration voltage of 10 kV,

primary ion beam current of 200 mA, and sputtered area of 150 by 150 um were selected. Gold coating was applied on the specimen surface with 300Å thickness to reduce the charge effect of Zircornia and an electron gun was used to eliminate the stored charge during the analysis. In SIMS depth analysis, secondary ion counts were indicated as a function of sputtering time. The crater depth was measured by surface roughness tester (α -step 300) to convert sputtering time into oxide depth. Oxide thickness was also measured by metallography, and the depth measured by the roughness tester was calibrated. Secondary ion counts were converted into the function of oxide depth based on those measurements.

TEM studies on the oxide formed in LiOH, NaOH, and KOH and SEM studies at the metal/oxide interface were carried out. To accurately investigate the characteristics of oxides formed in various solutions, the specimens with an equal oxide thickness should be prepared. If autoclave tests are conducted for a constant exposure time, the different oxide thickness is obtained in each solution due to the different corrosion rates. Therefore, in this study, the different exposure time was applied for each sample depending on solutions to obtain the corroded specimens with the weight gain of 25 mg/dm^2 in pre-transition regime and the weight gain of 60 mg/dm^2 in post-transition regime. TEM specimens for the observation of oxide microstructures were prepared in a sequence of cutting, grinding, and polishing. Finally thin foil was prepared by Ar ion milling.

The morphologies of oxide at the oxide-metal interface after the corrosion tests were observed using scanning electron microscope (SEM) after dissolving completely the metal part with a mixing solution of 10% HF, 45% HNO_3, and 45% H_2O. The amounts of hydrogen pickup in the corroded specimens were also quantitatively analyzed by using the hot extraction method and hydrogen analyzer (LECO Co.). Before hydrogen analysis of corroded specimens, the oxide films were removed by sand blasting.

3. Results

3.1. Long-term corrosion in LiOH, NaOH, KOH, RbOH, and CsOH solutions

Fig.1 to 5 shows the corrosion behaviors of Zr-based alloys in LiOH, NaOH, KOH, RbOH, and CsOH solutions at 350℃ for 500 days. In the previous study[11], the corrosion evaluation of Zircaloy in alkali hydroxide was not clearly performed due to the short exposure time of 150 days. However, in the long-term corrosion test in this study, Zr alloys showed the corrosion behavior in the post-transition regime in all test conditions. As shown in Fig.1, in 4.3 mmol (30 ppm Li) LiOH solution, the Zircaloy showed the transition of corrosion rate at 100 days, and then its weight gain increased gradually with increasing exposure time. The Nb containing alloy, which is only a testing alloy, showed the early

transition of the corrosion rate at 50 days compared to Zircaloy. In 32.5 mmol (220 ppm Li) LiOH solution, the both alloy exhibited the early transition and the significant acceleration of corrosion rate. This result is consistent with those by other investigators showing the accelerated corrosion in high concentration of LiOH.

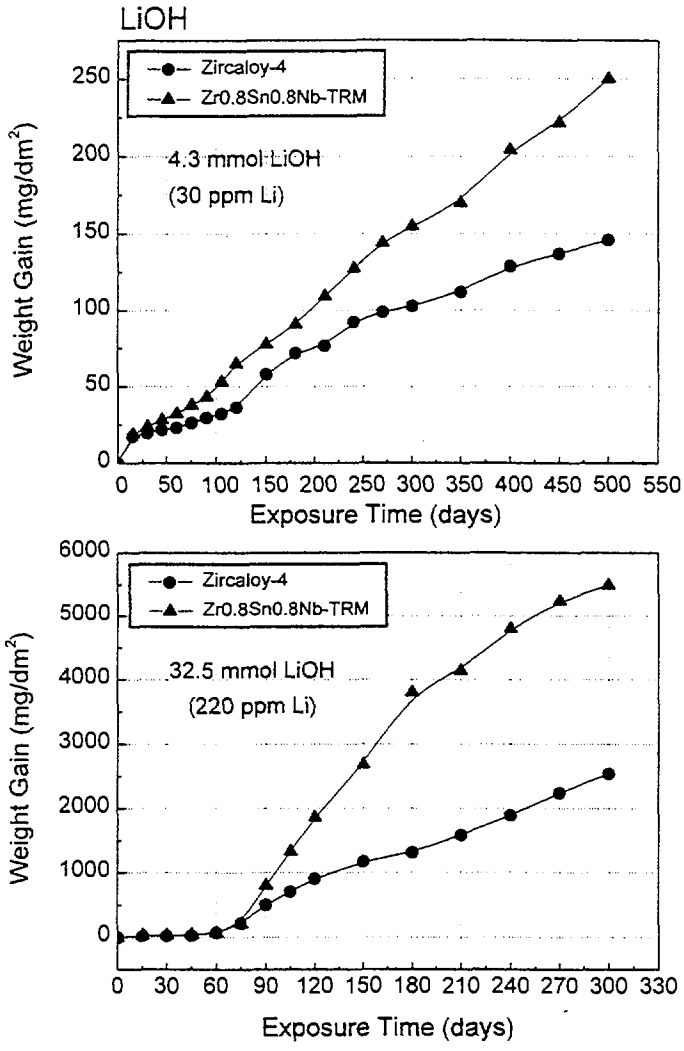

Fig.1 Corrosion behavior of Zr alloys in LiOH solutions at 350°C

The corrosion behavior in 4.3 mmol NaOH solution is similar to that in 4.3 mmol LiOH solution as shown in Fig. 2. However, the corrosion behavior in 32.5 mmol NaOH solution is quite different to that in 32.5 mmol LiOH solution. The Nb containing alloy in 32.5 mmol NaOH showed the oxide spalling at 200 day exposure time with weight gain of 150 mg/dm^2. This oxide spalling was not observed on the sample corroded in 32.5 mmol LiOH solution even if its weight gain significantly increased up to 5500 mg/dm^2.

The corrosion behaviors in KOH (Fig.3), RbOH (Fig.4), and CsOH (Fig.5) were similar to that in NaOH regardless of the alloy composition and the concentration of alkali solution.

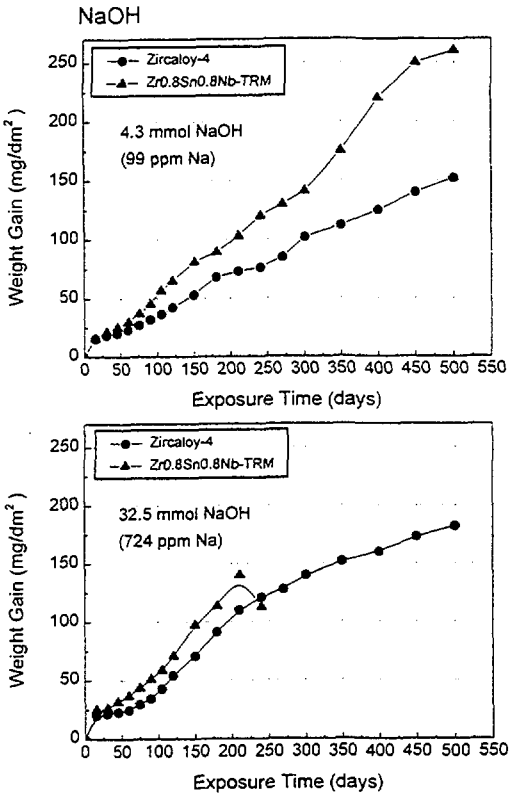

Fig.2 Corrosion behavior of Zr alloys in NaOH solution at 350°C

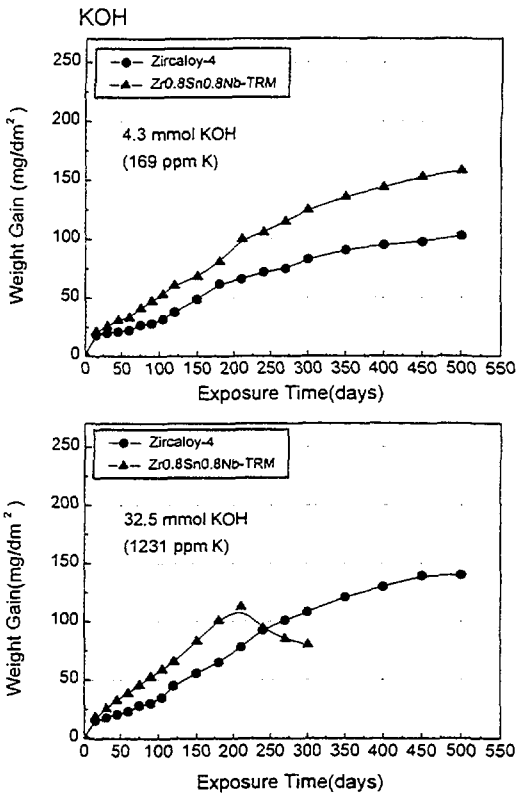

Fig.3 Corrosion behavior of Zr alloys in KOH solution at 350°C

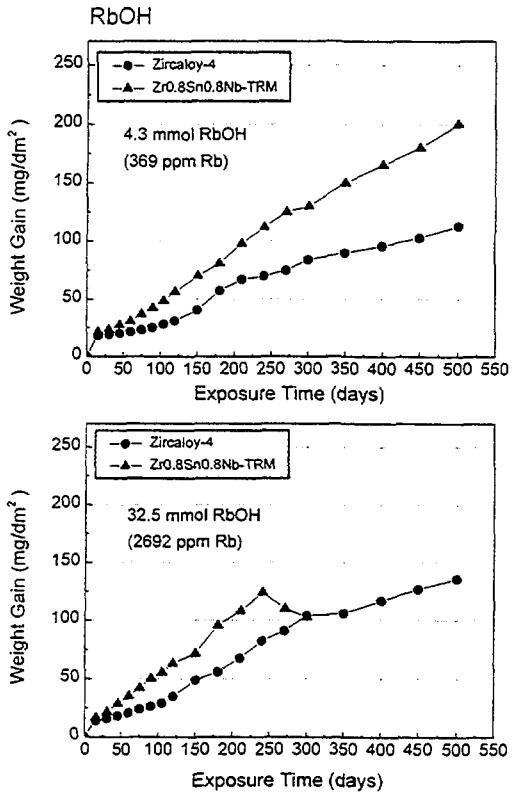

Fig.4 Corrosion behavior of Zr alloys in RbOH solution at 350°C

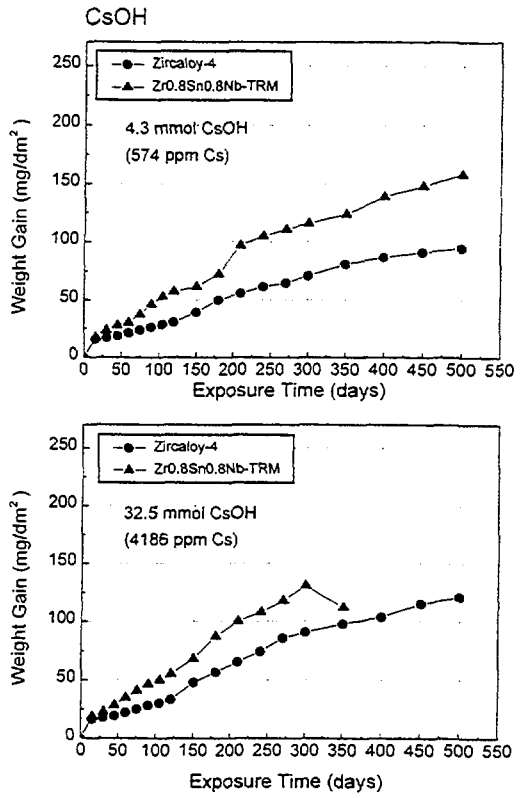

Fig.5 Corrosion behavior of Zr alloys in CsOH solution at 350°C

The oxide spalling of Nb containing alloy was also observed in KOH, RbOH, and CsOH with weight gain between 100 and 150 mg/dm^2. It is not clear whether the oxide spalling occurred only in Nb-containing alloys or in low corrosion resistant alloys. However, based on the Russian corrosion data showing the compatibility between KOH and Zr-1Nb cladding [17], it is considered that alkali hydroxides except LiOH can easily induce the oxide spalling in the low corrosion resistant alloys.

Fig.6 shows the weight gain after 500 days corrosion test as a function of ionic radius of alkali cation. In the concentration of 4.3 mmol, the weight gain decreased gradually with increasing the ionic radius of alkali cation up to 300 day. In the long-term test (500days), this trend is slightly changed in KOH and RbOH showing the fluctuation of corrosion rate, which would be caused by the reduced stability of oxide in NaOH and RbOH than in LiOH solution. In high concentration (32.5 mmol) of alkali hydroxide, the corrosion rate is

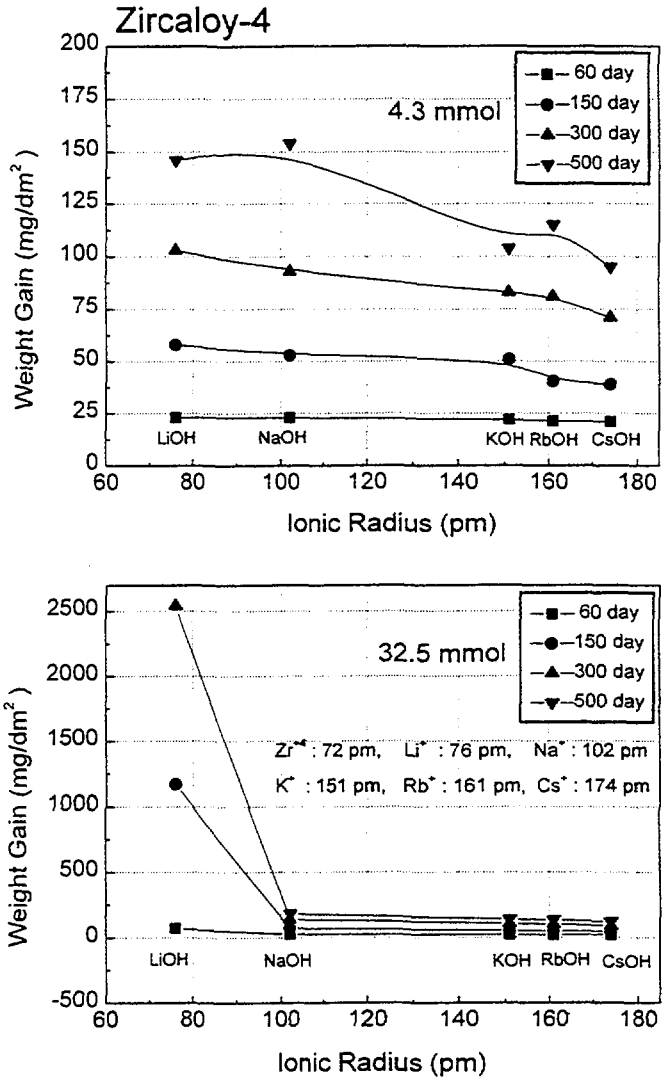

Fig.6 Weight gain of Zircaloy-4 as a function of alkali hydroxide cation

significantly accelerated in LiOH, where the ionic radius of Li^+ is similar to that of Zr^{4+} in the oxide. But the corrosion rate is not significantly accelerated in NaOH, KOH, and KOH solutions, where there is a big difference of ionic radius between cation and Zr^{4+} in the oxide. This means that there is a close relationship between the ionic radius of cation and the corrosion rate.

Fig. 7 shows the variation of hydrogen pickup fraction with the ionic radius. As the ionic radius of the alkali metal increases, the hydrogen pickup fraction decreases regardless of the concentration of alkali hydroxide. The hydrogen pickup fractions in high concentration of LiOH and NaOH increased compared to those in the low concentration. However, the hydrogen pickup fractions in the cases of KOH, RbOH, and CsOH solutions are almost the same showing about 15 % in both transition regimes. It means that the amounts of the hydrogen pickup and the hydrogen pickup fractions become high when the cation in an aqueous alkali hydroxide has a similar size to that of Zr^{4+}. Garzarolli [12] reported that the allotropic transformation of the oxide could be enhanced due to the mineralizing effect by the absorbed hydrogen during the corrosion, which results in accelerating the corrosion

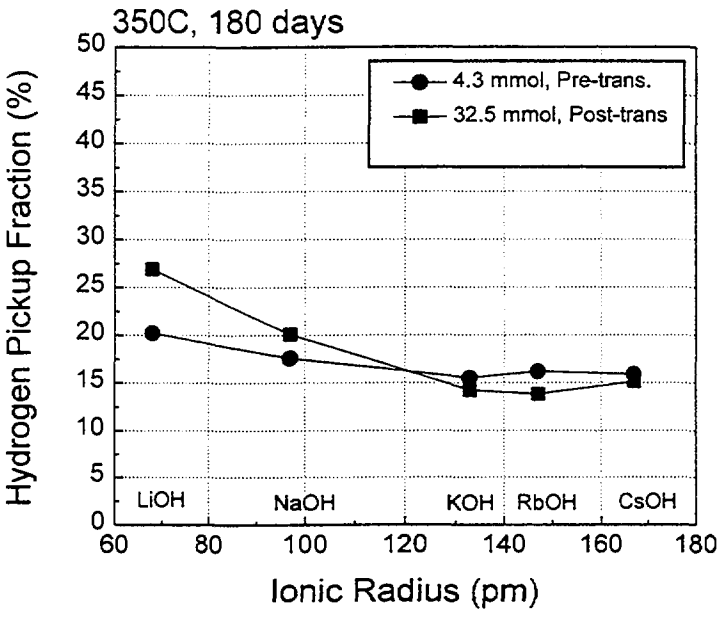

Fig.7 Hydrogen pickup fraction of Zircaloy-4 in equimolar alkali hydroxide solution

3.2. Cation content in the oxide by chemical analysis and SIMS

The cation contents in the oxide were measured by SIMS and chemical analysis. Fig.8 shows the cation contents in the oxide by chemical analysis with a variation of weight gain as a function of ionic radius of cation in 4.3 mal solutions. The cation contents decreased gradually with increasing the ionic radius from Li^+ to Cs^+. This variation of cation content is

consistent with that of weight gain. Therefore, it can be thought that the corrosion in low concentration of alkali hydroxides would be controlled by the cation incorporation into the oxide. However, in the high concentration of alkali hydroxides, the variation of cation content in the oxide showing a slight decrease between LiOH and NaOH is inconsistent with that of weight gain showing a rapid decrease. Therefore, it is thought that the strong acceleration of corrosion rate in high concentration of LiOH would be controlled not only by the cation incorporation but also by other factor like oxide microstructure.

Fig. 9 shows the oxide thickness formed in 32.5 mmol LiOH, NaOH, and KOH for 300days. The oxide thickness in LiOH, NaOH, and KOH was about 150, 9, and 6μm, respectively. These samples were used for SIMS analysis.

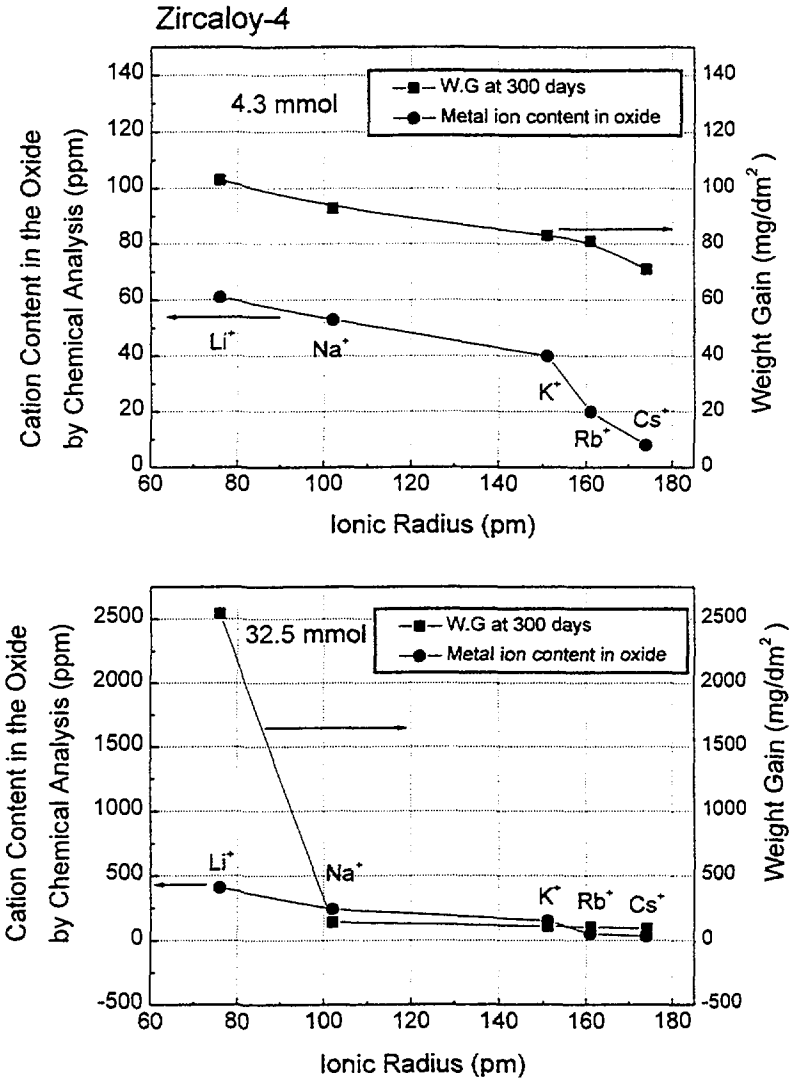

Fig.8 Variation of cation content in the oxide by chemical analysis with increasing the ionic radius of alkali hydroxide cation

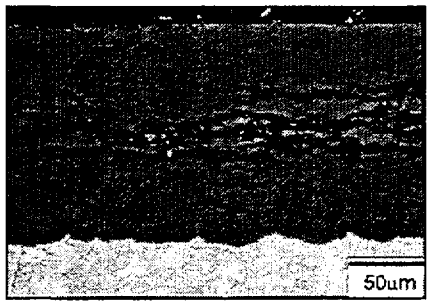

(a) LiOH

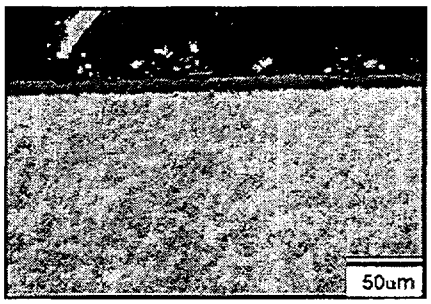

(b) NaOH

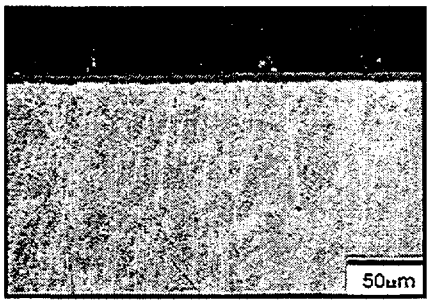

(c) KOH

Fig.9 Oxide Thickness of Zircaloy-4 corroded in 32.5 mmol LiOH, NaOH, and KOH for 300days

Fig.10 shows the depth profile of Li^+, Na^+, and K^+ by SIMS analysis on the oxide formed in high concentration of alkali hydroxide as a function of distance from the oxide surface. The Li^+ profile rapidly decreased from the oxide surface to 1μm, and then maintained constant up to long distance. The oxide thickness in LiOH solution was too thick to measure the Li^+ profile at metal-oxide interface. The Na^+ profile by SIMS shows rapid decrease from surface to 0.5μm, flat concentration to 3μm, and rapid decrease again. On the oxide formed in KOH solution, the content of K^+ ion continuously decreased up to 2μm without a flat region. The penetration depth of cation decreased in order of Li^+, Na^+, and K^+ ion. However, the fraction of penetration depth from total layer was not clearly evaluated because each oxide thickness was quite different in the corroded samples used for SIMS analysis.

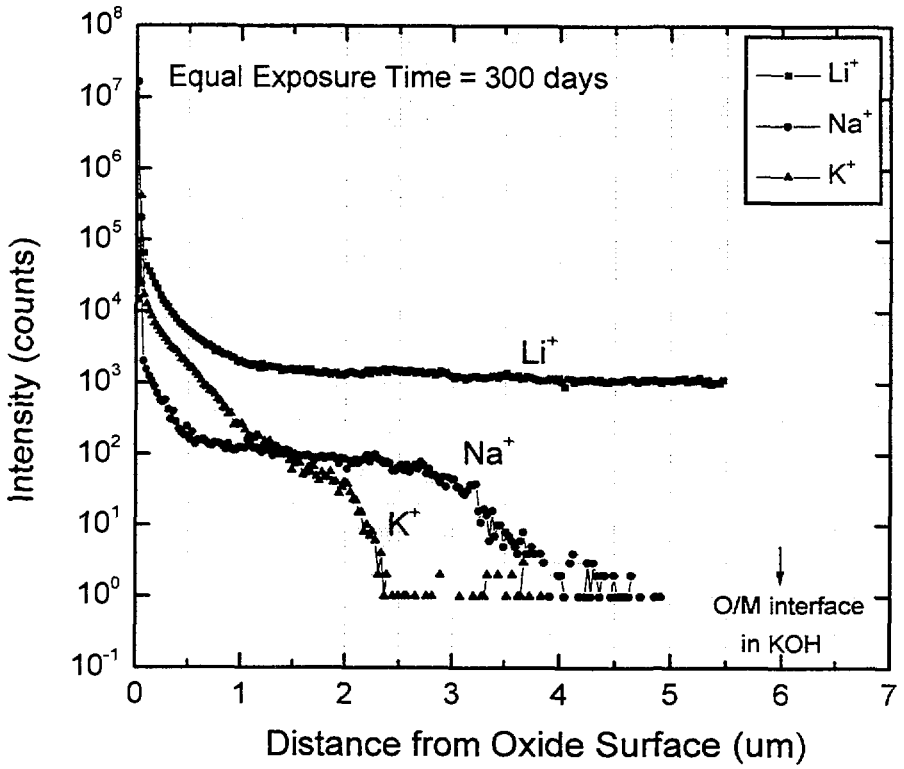

Fig.10 SIMS depth profile of Li^+, Na^+, and K^+ in the oxide formed during long-term autoclave test in 32.5 mmol alkali hydroxide solution

3.3. TEM and SEM microstructure of the oxide formed in LiOH, NaOH, and KOH

The TEM observation was performed on the oxide formed in LiOH solution as shown in Fig.11. The oxide in the pre-transition regime as well as the post-transition regime is composed of equiaxed structure. This structure is also observed at the metal-oxide interface of oxide grown in both regimes. Other investigators [13,18] reported that the oxide structures were transformed from the columnar grains in pre-transition regime to the equiaxed grains in post-transition regime. However, in this study the columnar grain was not observed even in pre-transition region, which means that the columnar grain was not formed or not maintained for such exposure time due to the high corrosion rate in LiOH solution even if it was formed. The grain sizes of oxides are measured as 15-20 nm in pre-transition regime (Fig.11-a) and 20-25 nm in post-transition regime (Fig.11-b). Many white grain boundaries are observed in the oxides formed in pre-transition as well as in post-transition regime. It was reported by Pêcheur[13] and Beie[19] that the white grain boundaries would be open grain boundaries or pores which indicates the weak intergranular cohesion.

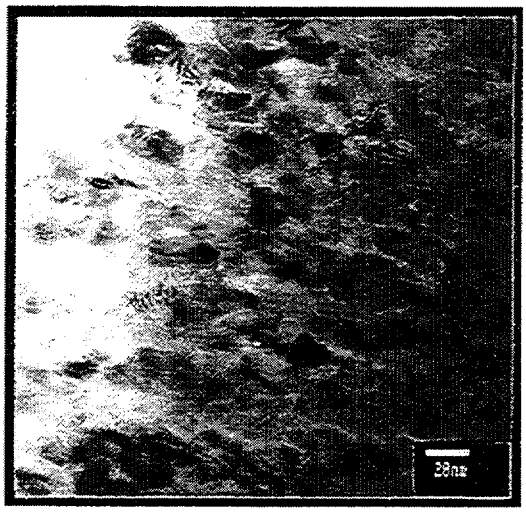

(a)

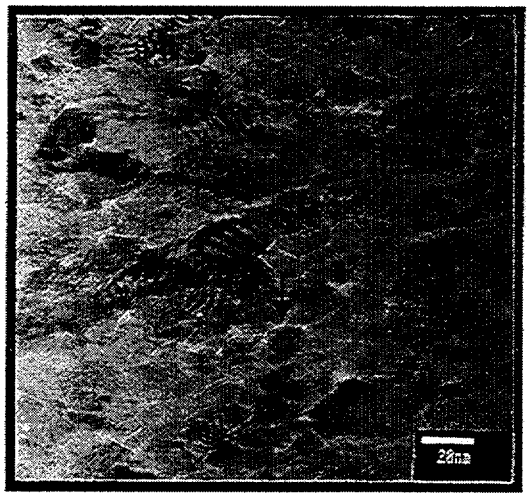

(b)

Fig.11 Cross-sectional TEM micrographs of Zircaloy oxide grown in LiOH solution (a) pre-transition (25mg/dm^2) (b) post-transition (60mg/dm^2)

Fig.12 shows the TEM micrographs on the oxide formed in NaOH solution. In pre-transition regime the columnar grains with the length of 150-200 nm and the width of 15-20 nm are observed. Even if the corroded samples have an equal oxide thickness in LiOH and NaOH, the columnar grains are observed only in the oxide formed in NaOH solution. The preservation of the columnar grains in NaOH solution would be related to the low corrosion rate in NaOH solution as compared with that in LiOH solution. Nevertheless, in post-transition regime the columnar grains are transformed into the small equiaxed grains with the grain size of 15-20 nm including the many open grain boundaries or pores.

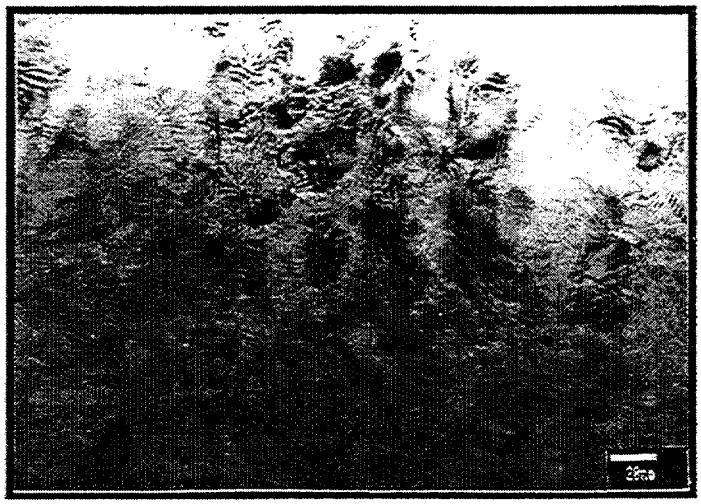

(a)

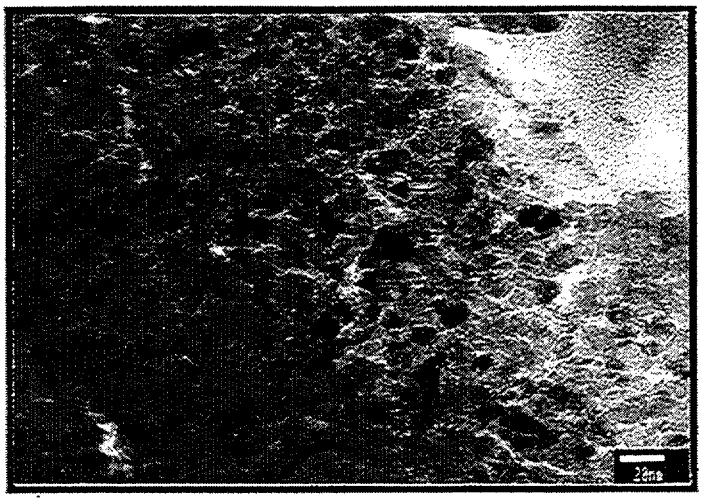

(b)

Fig.12 Cross-sectional TEM micrographs of Zircaloy oxide grown in NaOH solution (a) pre-transition (25mg/dm^2) (b) post-transition (60mg/dm^2)

The TEM microstructures of the oxide formed in KOH solution are shown in Fig.13. The oxide formed in pre-transition regime is mostly composed of the columnar grains. This means that the oxide formed in KOH solution is more protective and stable than those formed in LiOH and NaOH solutions.

The SEM micrographs at the metal-oxide interface of the Zircaloy-4 sheet corroded in LiOH, NaOH, and KOH solutions were shown in Fig.14. The oxide morphologies grown in the post-transition regime of LiOH solution represent the shape of ice columns having the different orientation of the oxide growth and the different growth rate of the oxide with varying the grain orientation of metal. It is observed that the oxide morphologies at the

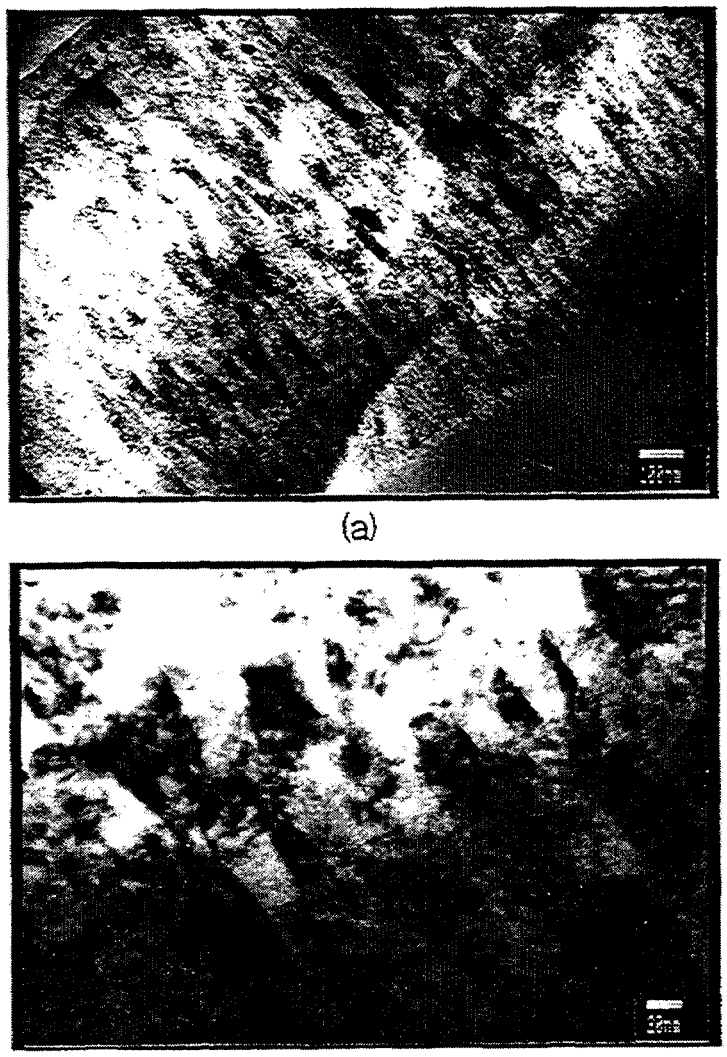

Fig.13 Cross-sectional TEM micrographs of Zircaloy oxide grown in KOH solution (a) pre-transition (25mg/dm^2) (b) post-transition(60mg/dm^2)

metal-oxide interface are different from grain to grain of the zirconium matrix. It is also observed that the corrosion rate at the grain boundary of zirconium matrix is much faster than that at the interior of the zirconium matrix grain. In the long-term corrosion test for 200 days in LiOH solution, the ice columnar oxides are transformed into the cauliflower morphologies containing the numerous open pores and cracks between the lump-type oxides. The oxides formed in post-transition regime of NaOH solution show the remarkable difference in the oxide morphology with varying the grain orientation of zirconium metal. The width of ice columnar oxides in NaOH solution is much narrower than that in LiOH solution. After a long-term corrosion test for 200 days in a NaOH solution, the ice columnar oxides are mainly transformed into the lump-type oxides but still remained with small fraction. In particular, the cauliflower morphologies of oxides are not observed even after a

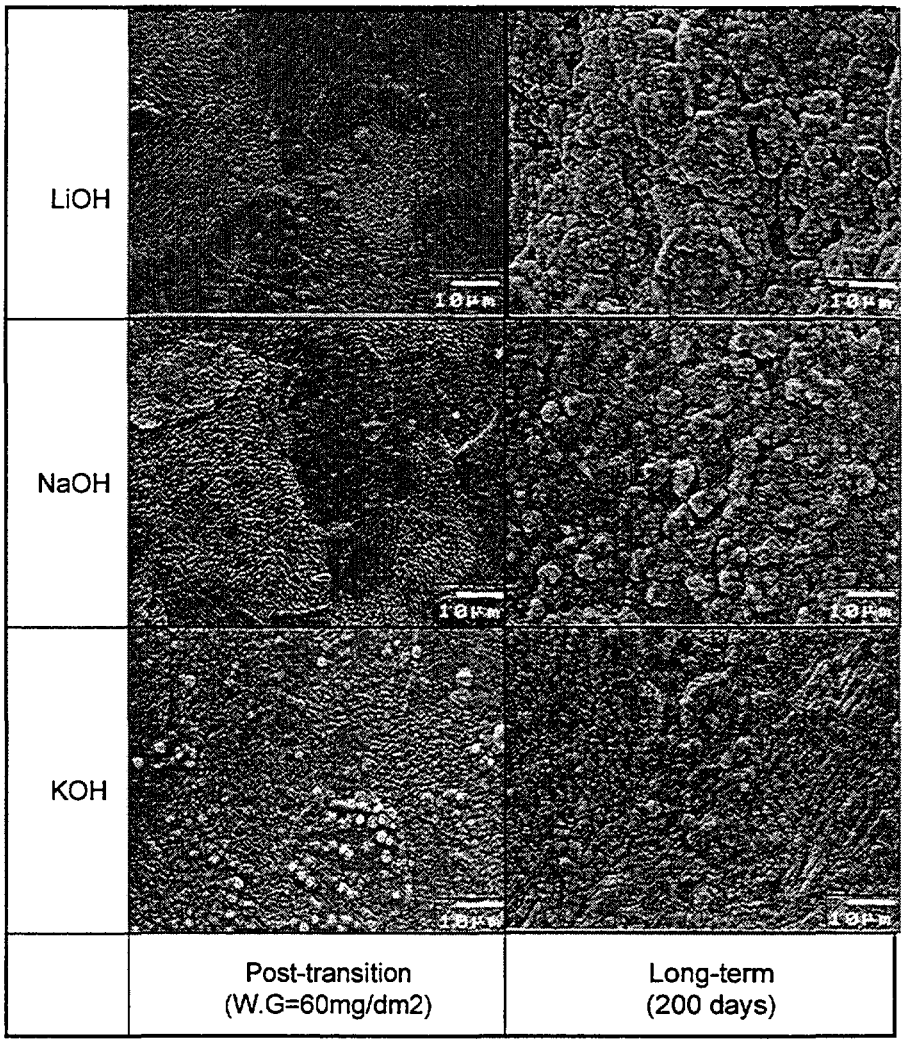

Fig.14 SEM micrographs at metal-oxide interface of Zircaloy-4 in LiOH, NaOH, and KOH solution

long-term corrosion test in NaOH solution. In KOH solution, the process of oxide development is quite different from those in LiOH and NaOH solution. The numerous small round-type oxides, instead of ice columnar oxides, are formed in the post-transition regime. After a long-term corrosion test in KOH solution, the round-type oxide is replaced by the mixed oxides of a columnar-type in a major portion and round-type in a minor portion.

4. Discussion

Based on the corrosion characteristics, the SIMS analysis, and the oxide microstructure, the discussion is classified into the two mechanistic aspects; one is related to the slight enhancement in low concentration and in pre-transition regime of high concentration, and the other the significant enhancement in high concentration.

The corrosion result in low concentration (4.3mmol) of alkali hydroxide shows that the corrosion rate decreases gradually with an increasing ionic radius of alkali cation. This

phenomenon would be caused by the difference of ionic radius between cation and Zr^{4+}. It would be easy to substitute Li^+ for Zr^{4+} in the oxide layer due to the similar ionic radii (Li^+ =76 pm and Zr^{4+} =72 pm) whereas it be very difficult for Na^+, K^+, Cs^+, and Rb^+ to do due to the big difference of ionic radius between cation and Zr^{4+}. Also, it can be said that the slight enhancement of corrosion rate in LiOH solution is induced owing to the easy substitution of Li^+ for Zr^{4+} in the oxide layer, indicating the formation of many anion vacancies, by the similar size of their ionic radii. This hypothesis is supported by the variation of cation concentrations measured in this study, namely, the gradual decrease of cation concentration with an increasing ionic radius of cation. Therefore, the slight enhancement of corrosion rate in low concentration of LiOH would be controlled by Li^+ incorporation into the oxide. However, the significant acceleration that occurred in the long-term corrosion test of more than 500days in low concentration can not be explained by this hypothesis. Other factors like oxide characteristics may affect the significant acceleration of corrosion.

It was observed from the corrosion tests in equimolar alkali hydroxides that the corrosion rate of Zircaloy-4 was dependent on the alkali hydroxide. Therefore, the effect of OH^- ion in the aqueous solution on the corrosion could be excluded by the equimolar M^+ and OH^- condition used in this study. It could be suggested that the corrosion of the Zircaloy-4 in alkali hydroxide solutions be accelerated by the existence of metallic ion, not by the OH^- ion (or pH).

Regarding the corrosion behaviors in high concentration of alkali hydroxide, in the pre-transition region, the corrosion behaviors showed the gradual decrease with increasing the ionic radius. The SIMS analysis on the samples showed that the penetration depth decreased and the ratio of barrier layer to total layer increased with increasing the ionic radius of cation. Even in high concentration of alkali hydroxide, the corrosion behavior in pre-transition regime is well consistent with the depth of the barrier layer in the oxides formed in LiOH, NaOH, and KOH solution. Therefore, it is thought that the corrosion in pre-transition regime of high concentration would be controlled by the cation incorporation. In the post-transition regime of high concentration, it was observed that corrosion rate was significantly accelerated in only LiOH but slightly in other alkali hydroxides. The cation concentration in the oxide by chemical analysis decreased gradually with increasing the ionic radius. Therefore, the cation concentration in the oxide is not clearly consistent with the corrosion behaviors in alkali hydroxide solutions. In SIMS analysis on the thick oxide formed in LiOH, NaOH, and KOH solution for 300days, it was observed that Li^+ could be penetrated to the very long distance but Na^+ and K^+ up to only 3 and 2 μm, respectively. Therefore, from the corrosion behavior in high concentration and the cation content by SIMS and chemical analysis, it is considered that the strong acceleration of the corrosion rate in high concentration would be caused by not only cation incorporation but also other factors.

It was investigated from the TEM study on oxide that, even if they have an equal oxide thickness, the oxide morphologies are quite different depending on the alkali hydroxide. In LiOH solution the equiaxed structure was formed in both regimes of pre-and post-transition, in NaOH solution the columnar structure in pre-transition and the equiaxed structure in post-transition regime, and in KOH solution the columnar structure in both transition regimes. From the above results, it is thought that the cation in alkali hydroxide can affect the oxide characteristics including morphology, growth mechanism, and spalling of oxide.

In a high concentration of alkali hydroxide solution, LiOH accelerates the corrosion due to the early transformation of oxide morphology from columnar to equiaxed structure. On the other hand, KOH is effective to maintain stable oxide morphology. Therefore, the strong acceleration of corrosion in high concentration of LiOH is mainly caused by the transformation of the oxide microstructure, which would be resulted from the cation incorporation in the oxide. However, it is not clear in this study how the cation incorporation induces the transformation of oxide microstructure.

KOH, which is being used as a pH controller with other alkali hydroxide in WWER reactor, does not significantly accelerate the corrosion and the hydrogen pickup of Zircaloy. Thus, KOH has a potential as an alternative alkali hydroxide for PWR reactors. However, the systematic study to use the KOH for PWR reactor is necessary because, according to Henzel's paper [20], KOH may induce the stress corrosion cracking in other primary components.

5. Conclusions

The results from the long-term corrosion test, SIMS analysis, and oxide study lead to the following conclusions;

1. The corrosion rate in alkali hydroxide solutions decrease with the increasing ionic radius of alkali cation. The cation would control the corrosion in alkali hydroxides with equimolar M^+ and OH^-. The effect of cation on the corrosion is dependent on the alkali concentration and the oxide thickness.

   -The slight enhancement of corrosion in low concentration is controlled by the cation incorporation into oxide, which results in the increase of anion vacancy and the decrease of the barrier layer.

   -The strong acceleration of corrosion in high concentration is mainly controlled by the transformation of oxide microstructure, which would be caused by the cation incorporation into oxide.

2. KOH does not significantly accelerate the hydrogen pickup as well as the corrosion rate of Zircaloy even in a high concentration. It is thought that KOH has a potential as an alternative alkali for PWR application with respect to Zircaloy corrosion.

REFERENCES

[1] F.GARZAROLLI, J.POHLMEYER, S.TRAPP-PRITSCHING, H.G.WELDINGER, "Influence of various additions to water on Zircaloy-4 corrosion in autoclave tests at 350°C", Fundamental Aspects of Corrosion on Zirconium Base Alloys (Proc. Mtg Portland, Oregon, USA, 1989), Rep. IWGFPT/34, IAEA (1990) 65.

[2] S.G.MCDONALD, G.P.SABAL AND K.D.SHEPPARD, "The effect of lithium hydroxide on the corrosion behaviour of Zircaloy-4", Zirconium in Nuclear Industry (Proc. 6th Int. Symposium, Vancoever, BC, Canada, 1984), ASTM, ASTM STP 824 (1984) 519.

[3] E.HILLNER AND J.N.CHIRIGOS, "The effect of lithium hydroxide and related solutions on the corrosion rate of Zircaloy-2 in 680°F water", US Report WAPD-TM-307, Bettis Atomic Power Laboratory, W. Mifflin, PA (1967).

[4] R.A.PERKINS AND R.A.BUSCH, "Corrosion of Zircaloy-4 cladding", Environmental Degradation of Materials in Nuclear Reactor Systems (Proc. 4th Int. Symposium Jekill RIsland, GA, USA, 1990, ASTM, ASTM STP 1132 (1991) 595

[5] I.L.BRAMWELL, P.D.PARSONS, AND D.R.TICE, "Corrosion of Zircaloy-4 PWR fuel cladding in lithiated and borated water environments", Zirconium in Nuclear Industry (Proc. 9th Int. Symposium, Kobe, Japan, 1990), ASTM, ASTM STP 1132 (1991) 628.

[6] N. RAMASUBRAMANIAN AND P.V.BALAKRISHNAN, "Aqueous chemistry of lithium hydroxide and boric acid and corrosion of Zircaloy-4 and Zr-2.5%Nb", Zirconium in Nuclear Industry (Proc. 9th Int. Symposium, Kobe, Japan, 1990), ASTM, ASTM STP 1132 (1991) 628.

[7] N.RAMASUBRAMANIAN, N.PRECOANIN, AND V.C.LING, " Lithium uptake and the accelerated corrosion of zirconium alloys", Zirconium in Nuclear Industry (Proc. 8th Int. Symposium, San Diego, USA, 1988), ASTM, ASTM STP 1023 (1989) 187.

[8] N.RAMASUBRAMANIAN, "Lithium uptake and corrosion of zirconium alloys in aqueous lithium hydroxide solutions", Zirconium in Nuclear Industry (Proc. 9th Int. Symposium, Kobe, Japan, 1990), ASTM, ASTM STP 1132 (1991) 613.

[9] B.COX AND C.WU, "Dissolution of zirconium oxide film in 300°C LiOH", J. Nucl. Mater. **199** (1993) 272.

[10] B.COX, M. UNGURELU, Y.M.WONG, AND C.WU, "Mechanism of LiOH and H_3BO_3 repair of ZrO_2 film", Zirconium in Nuclear Industry (Proc. 11th Int. Symposium Germany, 1995), ASTM, ASTM STP 1295 (1996) 114.

[11] Y.H.JEONG, H.RUHMANN AND F. GARZAROLLI, IAEA-TECDOC-972, ""Influence of alcali metal hydroxides on corrosion of zirconium-based alloys" (Proc. Mtg Rez, Czech Republic, 1993), IAEA-TECDOC-927 (1997) 161.

[12] F.GARZAROLLI, H.SEIDEL, R.TRICOT, AND J.P.GROS, "Oxide growth mechanism on zirconium alloys", Zirconium in Nuclear Industry (Proc. 9th Int. Symposium, Kobe, Japan, 1990), ASTM, ASTM STP 1132 (1991) 395.

[13] D.PÊCHEUR, J.GODLEWSKI, P.BILLOT, AND J.THOMAZET, "Microstructure of oxide films formed during the waterside corrosion of the Zircaloy-4 clading into lithuated environment", Zirconium in Nuclear Industry (Proc. 11th Int. Symposium Germany, 1995), ASTM, ASTM STP 1295 (1996) 94.

[14] D.PECHEUR, A.GIORDANO, E.PICARD, PH.BILLOT, AND J.THOMAZET, "Effect of elevated lithium on the waterside corrosion of Zircaloy-4: experimental and predictive study", Influence of Water Chemistry on Fuel Cladding Behavior (Proc. Mtg Rez, Czech Republic, 4-8 October, 1993), IAEA-TECDOC_927 (1997) 111.

[15] D.PECHEUR, J.GODLEWSKI, J.PEYBERNES, L.FAYETTE, M.NOE, A.FRICHET, AND O.KERREC, "Contribution to the understanding of the effect of the water chemistry on the oxidation kinetics of Zircaloy-4 cladding", Zirconium in the Nuclear Industry, (Proc. 12th Int. Symposium Toronto, Canada, 1998), ASTM, ASTM STP1354 (in press).

[16] T.KIDO, S.WADA, T.TAKARASHI, H.UCHIDA, I.KOMINE, AND Y.INOUE, "Behaviour of lithium and boron in irradiated and unirradiated oxides formed on Zircaloy-4 claddings", Zirconium in the Nuclear Industry, (Proc. 12th Int. Symposium Toronto, Canada, 1998), ASTM, ASTM STP1354 (in press).

[17] J.KYSELA, M.ZMITKO, AND V. VRTILKOVA, "VVER water chemistry related to fuel cladding behaviour" (Proc. Mtg Rez, 1993), IAEA-TECDOC-972 (1997) 473.

[18] H.ANADA AND K.TAKEDA, "Microstructure of oxides on Zircaloy-4, 1.0Nb Zircaloy-4, and Zircaloy-2 formed in 10.3 Mpa steam at 673 K", Zirconium in Nuclear Industry (Proc. 11th Int. Symposium Germany, 1995), ASTM, ASTM STP 1295 (1996) 35.

[19] H.J.BEIE, A.MITWALSKY, F.GARZAROLLI, H.RUHMANN, AND H.J.SELL, "Examination of the corrosion mechanism of zirconium alloys", Zirconim in Nuclear Industry (Proc. 10th Int. Symposium, Baltimore, MD, USA, 1993), ASTM, ASTM STP 1245 (1994) 615-643.

[20] N.HENZEL, "Alternative water chemistry for the primary loop of PWR plants", Influence of Water Chemistry on Fuel Cladding Behaviour (Proc. Mtg Rez, 1993), IAEA, IAEA-TECDOC-972 (1997) 421.